Original Article

Impaired glymphatic system in patent foramen ovale based on diffusion tensor imaging analysis along the perivascular space

Liqiang Sun[1,2#^], Kaige Cui[1#], Jing Hu[1], Liqing Dong[3], Liying Liu[1], Juan Jia[1], Jiaqi Yu[1], Jiping Yang[1]

[1]Department of Medical Imaging, The Second Hospital of Hebei Medical University, Shijiazhuang, China; [2]Department of Radiology, Hebei General Hospital of Hebei Medical University, Shijiazhuang, China; [3]Department of Ultrasound, Hebei General Hospital of Hebei Medical University, Shijiazhuang, China

Contributions: (I) Conception and design: L Sun, J Yang; (II) Administrative support: K Cui, J Hu, J Yang; (III) Provision of study materials or patients: L Sun, K Cui; (IV) Collection and assembly of data: L Dong, L Liu; (V) Data analysis and interpretation: L Sun, J Jia, J Yu; (VI) Manuscript writing: All authors; (VII) Final approval of manuscript: All authors.

[#]These authors contributed equally to this work.

Correspondence to: Jiping Yang, PhD. Department of Medical Imaging, The Second Hospital of Hebei Medical University, No. 215 Heping West Road, Shijiazhuang 050000, China. Email: yangjiping@hebmu.edu.cn.

Background: Patent foramen ovale (PFO) is often complicated by cerebral diseases. Notably, PFO is disproportionately prevalent in cryptogenic stroke patients, but the mechanism of PFO is not clear yet. This study aimed to investigate whether there was a decline in the diffusion tensor imaging analysis along the perivascular space (DTI-ALPS) index that partially indicates interstitial fluid (ISF) dynamics and glymphatic system function in PFO patients, which had not been reported before, and to discuss the glymphatic metabolism mechanism by which PFO causes cryptogenic stroke.

Methods: In total, 52 PFO patients and 50 age- and gender-matched healthy controls (HCs) who underwent diffusion tensor imaging (DTI) with magnetic resonance imaging (MRI) scanning were included in the study. Diffusivity maps in the x-axis (D_{xx}), y-axis (D_{yy}), z-axis (D_{zz}), and the DTI-ALPS index from the projection and association fibers were extracted, and differences between PFO and HC groups were analyzed.

Results: The PFO patients had significantly higher D_{xx} and D_{yy} from the projection fibers, D_{zz} from the association fibers, lower DTI-ALPS indexes in both hemispheres, and higher D_{xx} from the association fibers in the left hemisphere than the HCs (P<0.01). The PFO patients had a lower DTI-ALPS index than the HCs in the left (1.358±0.116 *vs.* 1.624±0.281, P<0.001) and right (1.360±0.135 *vs.* 1.531±0.208, P<0.001) hemispheres. The areas under the receiver operating characteristic (ROC) curve were 0.83 with an ALPS index cut-off value of 1.434 in the left hemisphere, and 0.76 with an ALPS index cut-off value of 1.420 in the right hemisphere. Further, the paired samples *t*-tests revealed slight lateral differences in the DTI-ALPS index between the left and right hemispheres in the HCs (P=0.012). The reduced DTI-ALPS index of the left hemisphere (0.267±0.042) was greater than that of the right hemisphere (0.171±0.035).

Conclusions: The PFO patients showed a decrease in the DTI-ALPS index, which partly indicates ISF dynamic disorder and glymphatic system dysfunction, especially in dominant hemispheres. The DTI-ALPS index could serve as a neuroimaging biomarker for PFO. Further, the state of the impaired glymphatic system in PFO may increase the risk of stroke.

Keywords: Patent foramen ovale (PFO); glymphatic system; stroke; diffusion tensor imaging (DTI)

^ ORCID: 0000-0002-3280-1641.

Submitted Sep 16, 2024. Accepted for publication Feb 13, 2025. Published online Mar 19, 2025.
doi: 10.21037/qims-24-1963
View this article at: https://dx.doi.org/10.21037/qims-24-1963

Introduction

Patent foramen ovale (PFO) is the most common congenital intracardiac right-to-left shunt in adults (1). PFO affects about 25% of people, and is more common in individuals aged under 30 years (2). During the shunt process, the venous blood flows into the arterial circulation directly without pulmonary circulation, causing a series of diseases, including abnormal embolism, decompression sickness, and migraine (3,4). The prevalence of PFO in cryptogenic stroke patients is heterogeneous; about 25% of individuals have PFO (5). Notably, 29% of cryptogenic stroke patients have PFO, while only 20% of patients with a definite or probable cause of transient ischemic attack/stroke have PFO (5). The mechanism of PFO is not yet clear; thus, a deeper understanding of PFO pathophysiology is required.

Diffusion tensor imaging analysis along the perivascular space (DTI-ALPS) is a new, non-invasive method for evaluating glymphatic system function. This neuroimaging technology provides an objective means for investigating abnormal discoveries, and has been applied to many diseases, including Parkinson's disease (6), Alzheimer's disease (7), and epilepsy (8). The DTI-ALPS index is described as a crucial quantitative indicator for assessing the status of lymphatic metabolism (9), and a decrease in the DTI-ALPS index is an important parameter indicating a disordered condition of interstitial fluid (ISF) dynamics, which may partially suggest a dysfunction of the glymphatic system. To date, the glymphatic system function of PFO patients has not yet been explored. Thus, we used a DTI-ALPS technique to investigate whether a decline in the DTI-ALPS index which partially reflects (ISF) dynamics and glymphatic system function in PFO patients. We also discuss the lymphatic metabolic mechanism of PFO that causes cryptogenic stroke. We present this article in accordance with the STROBE reporting checklist (available at https://qims.amegroups.com/article/view/10.21037/qims-24-1963/rc).

Methods

The study was conducted in accordance with the Declaration of Helsinki (as revised in 2013). The study was approved by the Institutional Ethics Board of The Second Hospital of Hebei Medical University (No. 2023-R590), and informed consent was obtained from all the patients.

Participants

In total, 52 patients diagnosed with PFO at The Second Hospital of Hebei Medical University and 50 age- and sex-matched healthy controls (HCs) recruited from the community were enrolled in the study between September 2023 and August 2024 (*Figure 1*). All the participants underwent contrast transthoracic echocardiography, which served as the reference standard, and magnetic resonance imaging (MRI) scanning. Participants were included in the study if they met the following inclusion criteria: (I) were aged between 18 and 65 years; (II) were right handed; (III) had complete MRI data; and (IV) had not received medication and surgery to treat PFO. Participants were excluded from the study if they met any the following exclusion criteria: (I) had neurodegenerative diseases, tumors, or other neurological diseases; (II) had a long-term history of smoking, alcohol, or drug dependence; and/or (III) had poor-quality MRI scans.

Migraine assessment

In total, 52 patients completed the migraine symptom scale, which collects data on the frequency of migraine attacks per month, migraine duration, the visual analog scale (VAS), and the presence of accompanying symptoms.

MRI acquisition

The study used a 3.0 T MRI scanner (GE SIGNA Architect, USA) with a 24-channel head/neck coil. All participants lay still in a supine position. Earplugs were used to reduce noise, and foam cushions were used to decrease head motion. The diffusion tensor imaging (DTI) data were collected using a single-shot echo planar imaging sequence. The following parameters were used: repetition time (TR)/echo time (TE): 6,234/78.4 ms; b values: 0 and 1,000 s/mm^2; designed diffusion directions: 64; field of view: 256×256 mm; matrix size: 128×128; number of slices: 75; and slice thickness: 1.8 mm with no gap intersection.

DTI-ALPS index calculation

The DTI images were preprocessed based on the FSL pipeline on FMRIB 6.0 (FSL; https://fsl.fmrib.ox.ac.uk/fsl). First, the DICOM format data of the DTI images were converted to NIFTI by MRIcroN (https://www.nitrc.org/projects/mricron). Subsequently, eddy current and motion correction was performed. Skull stripping of the images was then performed. After which, fractional anisotropy (FA) and the diffusivity index toward the x-, y-, and z-axes in FSL were generated. Each FA map was then converted to the JHU-ICBM-FA template. The projection and association fibers were identified at the plane of the lateral ventricle body, the same as the superior longitudinal fasciculus (SLF) and the superior corona radiata (SCR) using the JHU-ICBM-DTI-81-white-matter-labelled Atlas. Regions of interest (ROIs) were outlined as 5 mm toward the bilateral SCR and SLF. The ROIs were centrally coordinated according to the JHU-ICBM-FA formwork, and fluid attenuated inversion recovery was used to try and exclude white-matter hyperintensities. Participants were excluded if the modified Fazekas scale for the white-matter hyperintensities was >2. Finally, the diffusivity index (D_{xx}, D_{yy}, and D_{zz}) was extracted to calculate the ALPS index. The ALPS index was defined as the ratio of the mean x-axis parameter along the projection direction (Dxxproj), and the x-axis diffusivity along the association fibers (Dxxassoc) to the mean of the y-axis parameter during the projection fibers (Dyyproj), and the z-axis parameter along the association direction (Dzzassoc) (9). The ALPS index was calculated using the following Eq. [1] (*Figure 2*):

$$ALPS\text{-}index = \frac{mean(Dxxproj, Dxxassoc)}{mean(Dyyproj, Dzzassoc)} \quad [1]$$

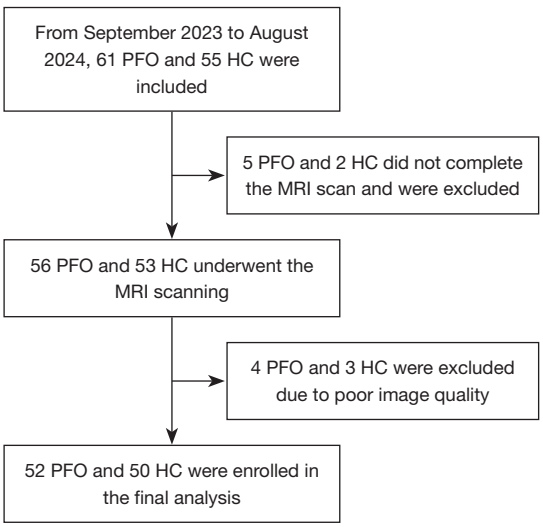

Figure 1 Study flow chart. HC, healthy control; MRI, magnetic resonance imaging; PFO, patent foramen ovale.

Statistical analysis

The participants' demographic and clinical data were compared using the independent sample *t*-test and Chi-squared test (GraphPad Prism, version 9.5.1). The DTI-ALPS index values between the left and right hemispheres were compared using the paired samples *t*-test. An analysis of covariance was used to analyze diffusivity parameters

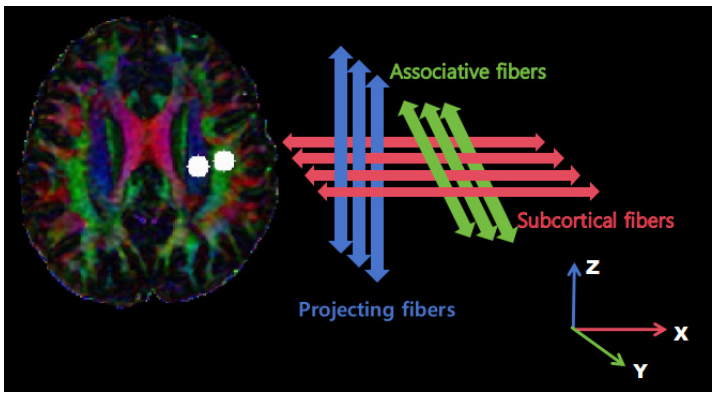

Figure 2 Calculation of the DTI-ALPS index in DTI color maps with ROIs from the projection fibers (blue as the z-axis), association fibers (green as the y-axis), and the subcortical direction (red as the x-axis). DTI-ALPS, diffusion tensor imaging analysis along the perivascular space; ROI, region of interest.

with the ALPS index, age, gender, body mass index (BMI) as co-variates, and the results were corrected for multiple comparisons using false discovery rate correction. Pearson association was analyzed in the ALPS index and migraine scores. The receiver operating characteristic (ROC) curve and the area under the curve (AUC) of the DTI-ALPS index between the groups were anal to identify the PFO patients compared to HCs. A P value <0.05 was considered statistically significant.

Results

Demographic data

In total, 52 PFO patients and 50 HCs were included in the study. There were no significant differences between the PFO group [mean ± standard deviation (SD): 39.62±9.706 years] and HC groups (mean ± SD: 39.64±10.565 years; P=0.990) in terms of age, sex (P=0.735), and BMI (P=0.526). For further details on the demographic data of the participants, see *Table 1*.

Table 1 Demographic and clinical data

Characteristic	PFO patients (n=52)	HCs (n=50)	P values
Age (years)	39.62±9.706	39.64±10.565	0.990
Sex (male/female)	14/38	12/38	0.735
BMI (kg/m^2)	21.306±1.729	21.518±1.626	0.526
Migraine scores	15.14±4.767	–	–

Data are presented as mean ± standard deviation or n. There were no significant differences between the PFO and HC groups in terms of their demographic data. BMI, body mass index; HCs, healthy controls; PFO, patent foramen ovale.

ALPS index and diffusion indices

There was a significant difference between the groups in terms of the ALPS index. Specifically, the PFO group had a lower ALPS index than the HC group in both the left (1.358±0.116 *vs.* 1.624±0.281, P<0.001) and right (1.360±0.135 *vs.* 1.531±0.208, P<0.001) hemispheres (*Figure 3*). Additionally, the D_{xx} and D_{yy} from the projection fibers, the D_{zz} from the association fibers in both hemispheres, and the D_{xx} from the association fibers in the left hemisphere were also significantly higher in the PFO patients than the HCs (*Table 2*). Further, the paired samples *t*-test results revealed a slight lateral difference in the DTI-ALPS index between the left and right hemispheres in the HCs according to (P=0.012). The reduced DTI-ALPS index of the left hemisphere (0.267±0.042) was greater than that of the right hemisphere (0.171±0.035), indicating a reduced lateral asymmetry in the PFO group.

The AUC of the ROC curve for differentiating between PFO and HC was 0.83 [95% confidence interval (CI): 0.75 to 0.91] using a sensitivity of 75% and specificity 76% by the ALPS index cut-off value of 1.434 in the left hemisphere and 0.76 (95% CI: 0.67 to 0.86) using a sensitivity of 77% and specificity 74% according to ALPS index cut-off value of 1.420 in the right hemisphere (*Figure 4*).

Correlation analysis

No significant correlation was found between the ALPS index and migraine scores (15.14±4.767, P=0.671).

Discussion

PFO has several neuropathological mechanisms. Paradoxical

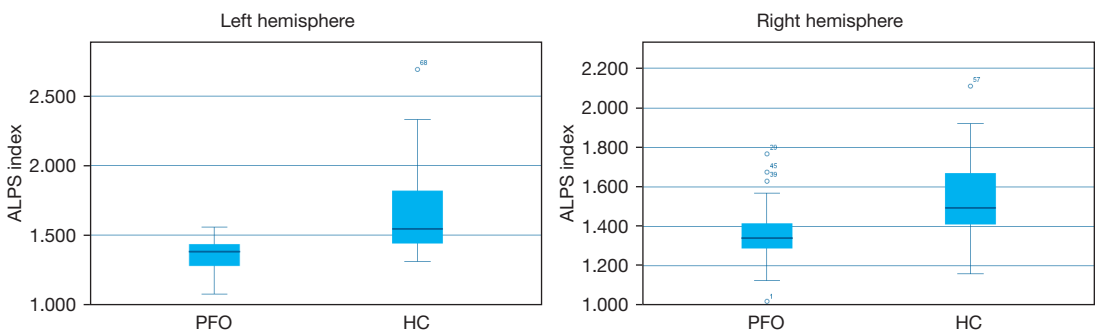

Figure 3 Difference in the ALPS index between the PFO and HC groups. ALPS, analysis along the perivascular space index; HC, healthy control; PFO, patent foramen ovale.

Table 2 Difference in the diffusivity parameters and the ALPS index between the PFO and HC groups

Characteristics	PFO group (n=52)		HC group (n=50)		P values
	Mean	SD	Mean	SD	
Left hemisphere					
Association fiber					
D_{xx} ($\times10^{-6}$ mm^2/s)	700.31	74.612	596.66	155.936	<0.001
D_{zz} ($\times10^{-6}$ mm^2/s)	423.48	51.106	309.70	125.204	<0.001
Projection fiber					
D_{xx} ($\times10^{-6}$ mm^2/s)	582.54	69.728	455.18	151.013	<0.001
D_{yy} ($\times10^{-6}$ mm^2/s)	523.62	61.099	357.12	114.079	<0.001
Left ALPS index	1.358	0.116	1.624	0.281	<0.001
Right hemisphere					
Association fiber					
D_{xx} ($\times10^{-6}$ mm^2/s)	672.37	73.988	620.92	173.108	0.052
D_{zz} ($\times10^{-6}$ mm^2/s)	417.62	59.324	342.52	159.093	0.002
Projection fiber					
D_{xx} ($\times10^{-6}$ mm^2/s)	562.56	58.276	470.60	183.157	0.001
D_{yy} ($\times10^{-6}$ mm^2/s)	495.92	70.186	394.64	145.588	<0.001
Right ALPS index	1.360	0.135	1.531	0.208	<0.001

ALPS, analysis along the perivascular space; D_{xx}, diffusivity through the x-axis; D_{yy}, diffusivity toward the y-axis; D_{zz}, diffusivity by the z-axis; HC, healthy control; PFO, patent foramen ovale; SD, standard deviation.

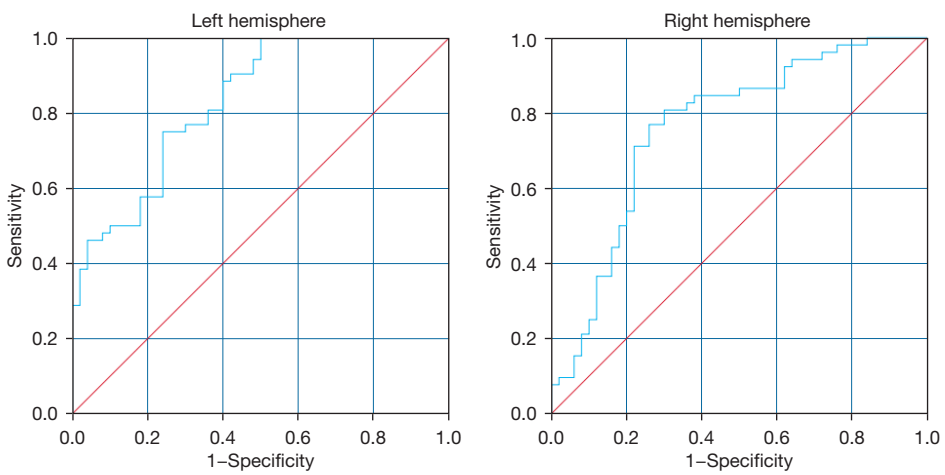

Figure 4 ALPS index ROC curve analysis for differentiating between PFO patients and HCs. The results revealed areas under the ROC curve of 0.83 (95% CI: 0.75 to 0.91) with a sensitivity of 75% and a specificity of 76% using an ALPS index cut-off value of 1.434 in the left hemisphere, and 0.76 (95% CI: 0.67 to 0.86) with a sensitivity of 77% and a specificity of 74% with an ALPS index cut-off value 1.420 in the right hemisphere. ALPS, analysis along the perivascular space; CI, confidence interval; HCs, healthy controls; PFO, patent foramen ovale; ROC, receiver operating characteristic.

embolism (PDE) occurs when venous thromboembolus flow into the arterial blood circulation through the foramen ovale, which may cause emboli in different parts of the body. If an embolism arrives at the brain, the cerebral arteries may be blocked, resulting in brain hypoxia, which in turn can lead to glymphatic and ISF exchange impairment, and even ischemia or infarction of the parenchyma if the embolism is large. Cerebral artery embolization often occurs in the posterior circulation due to faster blood flow velocity in the posterior circulation (10,11). However, a PFO itself may increase the blood circulation resistance, leading to the platelet aggregation and thrombus formation (12). Embolism-induced endothelial nitric oxide synthase (eNOS) expression in vascular endothelial cells appears to mediate blood-brain barrier (BBB) disruption, which can cause the abnormal leakage of large molecular substances, and a failure to clear extracellular waste, such as amyloid beta (Aβ), tau protein and lactate, resulting in ISF dynamic impairment and glymphatic dysfunction, which in turn can result in brain edema (13).

Most microparticle emboli via the PFO do not lead to cerebral infarction, but the ischemic state can trigger cortical spreading depression (CSD) (14). Depolarized neurons are supposed to decrease the efficiency of intra- and extracellular ion transportation, and disturb the metabolism of neurons. Additionally, CSD can induce the oligomerization through vasoconstriction, which may lead to abnormal changes in perivascular spaces called Virchow Robinson spaces, inducing damaged ISF exchange, resulting in localized hypoperfusion, which in turn can lead to various neurological symptoms (15,16). By activating special proteases, CSD can also change the permeability of the BBB, resulting in ISF dysfunction and leading to cerebral edema or hemorrhage (17). Additionally, CSD has the potential for dissemination, and focal ischemic areas can spread to non-ischemic areas in the form of waves, causing damage in distant parenchyma (18), which is most likely to occur in the hippocampus (19). CSD may also lead to impaired functional connectivity of both cerebral hemispheres (20).

Venous active factors [e.g., calcitonin gene-related peptide (CGRP), 5-hydroxytryptamine (5-HT), and endothelin] that should be eliminated in the pulmonary circulation are not decomposed, and flow directly into the cerebral circulation, affecting the function of cerebrovascular function (21,22); thus, the drainage of soluble waste along the perivascular spaces may break down, and they may act on neurons to cause a dural neurogenic inflammatory reaction (23). Neurogenic inflammation caused by the release of some active substances on the adjacent cerebral blood vessel wall after the stimulation of the trigeminal ganglion and its fibers manifests as BBB damage, plasma protein extravasation (PPE), or neurogenic vasodilatation. CGRP can activate and promote the degranulation of mastocyte in the dura mater, which leads to the release of CGRP, 5-HT, and other inflammatory mediators that aggravate the inflammatory response and form a positive feedback pathway of the inflammatory response (24), which in turn damages the basement membrane of capillaries and the tunica media of arteries, leading to obstacles in the exchange of ISF and the clearance of waste. Neuronal ischemic injury may be associated with 5-HT disorders (25). A previous study found that migraine patients with aura showed contrast media extravasation in the brain parenchyma after MRI enhancement, which suggests neurogenic inflammatory reaction (26).

When PDE occurs, venous blood with thrombus and 5-HT flows into cerebral arteries via the foramen ovale, which increases 5-HT concentration in the cerebral arteries, which in turn puts the blood in a hypercoagulable state, accelerates the formation of thrombosis, and increases the risk of PDE. The increased concentration of 5-HT may also induce CSD, and when combined with ischemia, damage to the brain parenchyma will be exacerbated (17,22). Guo *et al.* (27) revealed that these mechanisms may damage the cerebral blood autoregulation function in PFO patients, leading to metabolic waste clearance unbalance, which further causes migraine or stroke. Moreover, the larger the right-to-left shunt in the PFO, the more severe the impairment of the cerebral autoregulation function. This aligns with our findings that the ALPS index, as an indicator of glymphatic function, was significantly lower in the PFO group than the HC group.

To date, three cerebral lymphatic drainage systems, including the glymphatic system, the intramural periarterial drainage pathway, and the meningeal vessel lymphatic roads have been proposed (28,29). Iliff *et al.* first described the glymphatic system as a kind of precise anatomical and functional structure for the clearance of metabolites (30), including Aβ from neuronal metabolic activities, which are highly dependent on the aquaporin-4 (AQP4) of astrocytes. This pathway permits the cerebrospinal fluid (CSF) to flow in and the ISF to flow out, and maintains the homeostasis of the cerebral fluid (31). The intramural periarterial drainage pathway drains the waste across the basement membrane of capillaries and tunica media of arteries toward cervical

lymph nodes (32). Meningeal lymphatic vessels are able to clear ISF, immune cells, and macromolecules from the brain, and regulate the immune response (33). Of the above three pathways, the glymphatic pathway is the main method for clearing extracellular waste, such as Aβ (30), tau protein (34), and lactate (35). Additionally, the glymphatic system also contributes to molecules, such as cerebral glucose, amino acids, lipids, growth factors, and neuromodulators (36), which play crucial roles in brain metabolism. Notably, a lack of glucose leads to hypoxia of the brain parenchyma. Additionally, low glucose decreases the function of the BBB. Further, neurons cannot work properly if there is a lack of essential nutrients due to the reduction of amino acids.

Under the recent proposed "central nervous system interstitial fluidopathy" concept (37), abnormal ISF dynamics has a major association with the pathology. Flux fluid and macromolecules from the subarachnoid part rapidly enter the brain by bulk flow, via perivascular spaces called Virchow Robinson spaces. The term of "neurovasculome" was proposed by the American Heart Association/American Stroke Association, and is defined as the whole extracranial and intracranial vasculature, as well as the affiliated cells of the skull, meninges, and brain, including the arteries, veins, and the lymphatic system, neurovasculome plays a key role in brain homeostasis and cognitive health (38). The neurovasculome helps to convey metabolites and proteins from the parenchyma to the lymphatic system, and the draining mechanisms include transport through the BBB, the drainage of soluble waste along the perivascular spaces, and clearance by dual lymphatic vessels (39).

The role of the glymphatic system in the regulation of CSF-ISF exchange homeostasis is crucial, as an unbalance in the CSF-ISF exchange will exacerbate the formation of cerebral edema and hinder dissolution of the waste. Additionally, a decrease in glymphatic outflow drainage will increase the risk of vasogenic edema due to the impairment of AQP4 (40). Further, reduced tracer motion was detected in experimental models of brain amyloid angiopathy (41), even microinfarcts (42). Drainage disruption and the continued buildup of protein can result in the breakdown of vessel walls, leading to ischemic disease or hemorrhage. Glymphatic dysfunction can increase the permeability of the BBB, which suppresses responses of cerebral vessels to carbon dioxide (CO_2), which in turn leads to ischemic lesions (43).

Humans need stable cerebral blood flow (CBF) to meet the energy and metabolic demands of the brain. PDE caused by PFO leads to the concentration of emboli in blood and the blocking of cerebral arteries (11), and can further result in disorders of blood flow dynamics and ISF exchange. Guo *et al.* (27) revealed that these mechanisms may damage the cerebral blood autoregulation function in PFO patients, leading to metabolic waste clearance unbalance. Additionally, the increased resistance of blood by PFO could accelerate the expression of eNOS, which damages the BBB (13). Further, venous active factors as a result of PFO, such as CGRP, 5-HT, and endothelin, in the cerebral blood can affect vasoconstriction function (21,22) and even mediate vessel wall inflammation (24), exacerbating the damage to the BBB and ISF exchange dysfunction. The latest research suggests that neurons act as major organizers for the cerebral glymphatic system (44). CSD triggered by PFO disturbs the metabolism, and leads to the depolarization of neurons (16), which decreases CSF to ISF perfusion, leading to glymphatic dysfunction.

Several diseases, including Alzheimer's disease, Parkinson's disease (45), glioma (46), traumatic cerebral injury (47), subarachnoid hemorrhage, and ischemic stroke, have interstitial fluidopathy. AQP4 acts as the most vital glymphatic system and has a complicated action in cerebral edema after ischemia (48). Zhu *et al.* proposed that the glymphatic system is a key contributor to the formation of cerebral edema after ischemic stroke (49). Perivascular space enlargement and asymmetry could play a role in the glymphatic system, and can be visualized using advanced imaging methods after stroke (50). Lv *et al.* noted the potential of the glymphatic system in early risk assessment, diagnostics, and treatments, and stroke prognostics (51). The ALPS index revealed lower performance of ischemic stroke, indicating decreased glymphatic system function. The ALPS index increased from the onset of stroke, which indicated glymphatic function recovery (52). A longitudinal cohort study suggested that neurovascular coupling impairments after stroke lower glymphatic system function, and led to depressive symptoms (53). Keuters *et al.* discussed the effect of vascular endothelial growth factor C which caused a growth of dural lymphatic vessel on ischemic stroke, and noted that further investigations should be conducted to examine the effect of dural lymphatic system enhancement at clinically related temporal points (54).

This study found that the PFO patients had a significantly reduced DTI-ALPS index; thus, this index might be a good parameter for indicating disordered ISF dynamics and glymphatic dysfunction. We established ALPS index cut-off values of 1.434 in the left hemisphere

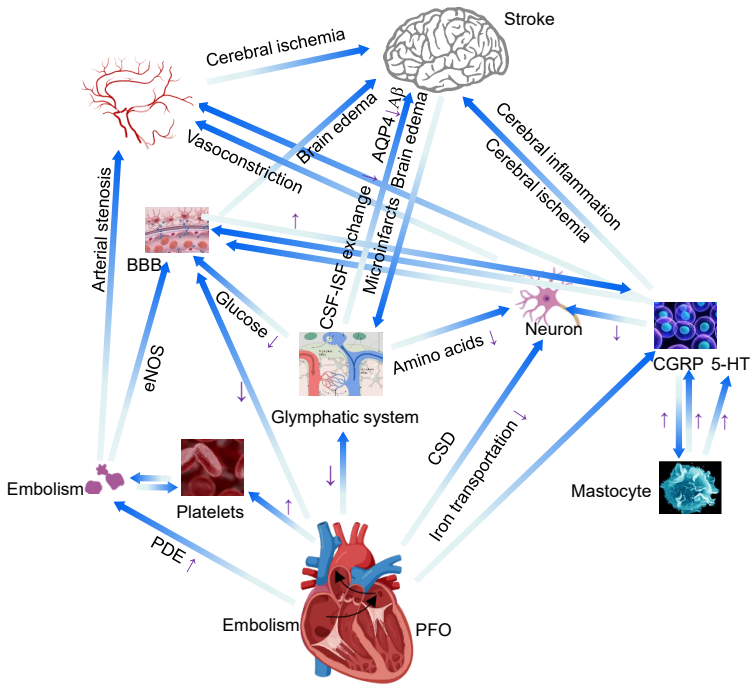

Figure 5 The relationship between the glymphatic system, PFO, and stroke. PFO can directly block cerebral arteries by the PDE pathway, leading to stroke. Increased resistance to blood circulation in PFO patients may lead to thrombus, which induces eNOS expression and disrupts the BBB. CSD can decrease ion transportation, causing the disturbance of neurons and vasoconstriction. Venous 5-HT and CGRP can directly flow into the cerebral blood, affecting the function of neurons, and even cause dural neurogenic inflammation. CGRP can activate mastocyte degranulation. The above process decreases the glymphatic function, and the homeostasis of CSF-ISF exchange can be broken, increasing BBB permeability and leading to ischemia. Further, the risk of vasogenic edema is increased because of the impaired AQP4. Conversely, cerebral ischemic stroke leads to glymphatic dysfunction, which is associated with brain edema. The arrow ↑ indicates an improvement in function or a quantitative increase, while the arrow ↓ indicates an inhibition in function or a reduction in quantity. AQP4, aquaporin-4; BBB, blood-brain barrier; CGRP, calcitonin gene-related peptide; CSD, cortical spreading depression; CSF, cerebrospinal fluid; eNOS, endothelial nitric oxide synthase; 5-HT, 5-hydroxytryptamine; ISF, interstitial fluid; PDE, paradoxical embolism; PFO, patent foramen ovale.

and 1.420 in the right hemisphere, which were effectively able to discriminate between PFO patients and HCs. Thus, the ALPS index could act as a potential biomarker for PFO. This study also examined the relationship between lymphatic metabolism, PFO, and stroke, and conjectured that the state of lymphatic metabolism dysfunction before stroke in PFO might have a mediating role between PFO and stroke (*Figure 5*).

The results of this study revealed slight lateral differences in the glymphatic system between the inter-hemispheres as evidenced by a greater DTI-ALPS index in the left hemisphere than the right hemisphere. It is well known that the left hemisphere is the dominant hemisphere in a majority of systems and functions. Cerebral function specialization and activation selection in specific brain regions that affect cognition and perception contribute to the evolution of the human brain (55). Thus, hemispheric lateralization plays a more critical role in one hemisphere, usually the left hemisphere (56), which offers an opportunity for optimizing brain efficiency and improving cognition (57). Recently, functional MRI research has shown hemispheric lateralization, especially in the dominant hemisphere, and even in the left frontal cortex based on blood oxygen level dependent (58). Thus, oxygen level contributes to the hemispheric dominance, leading to more severe hypoxia damage in the left hemisphere. Additionally, arterial spin labelling experiments also suggest that CBF distributions are asymmetric between inter-hemispheres (59), which means that the condition in the left hemisphere is more fragile. All of the above-mentioned studies reveal that the oxygen level

and perfusion between the inter-hemispheres differ, which may lead to lateral differences in glymphatic function. Our DTI-ALPS-based study confirmed the hypothesis that hemispheric dominance exists in the glymphatic system. Further, the dominant hemisphere (i.e., the left hemisphere) may be more fragile in PFO patients. A greater reduction of DTI-ALPS index in the left hemisphere compared to the right hemisphere led to reduced lateral asymmetry in the PFO group. The mechanisms of PDE, the ischemic state triggering CSD, and the expression of venous active factors might contribute to this process, and exacerbate the damage to the dominant hemisphere.

The DTI-ALPS index has been used as a crucial quantitative indicator to assess the status of lymphatic metabolism in recent years. In the radial direction at the ventricular body level, a higher DTI-ALPS index demonstrates the dominance of the Brownian motion of water molecules. Currently, several new perspectives about DTI-ALPS index exist. Taoka *et al.* were the first to report on the DTI-ALPS index, and noted that the decreased DTI-ALPS index as a good parameter indicates a disordered condition of ISF dynamics, which may partially suggest glymphatic system dysfunction (60). However, Ringstad is of the view that the DTI-ALPS should be examined critically (61). As suggested by basic science, the BBB and local proteolytic degradation may dominate the clearance process, and CSF-ISF exchange and glymphatic drainage may play a secondary role in deep white matter (62). Taoka *et al.* recommended using a combination of various methods, such as the intrathecal gadolinium-based contrast agent (GBCA) (63), intravenous GBCA (64), perivascular space volume (65), and choroid plexus volume (66), to evaluate the glymphatic system. Doing so, may provide us with more methods and indicators for examining the glymphatic system of humans.

Limitations and prospects

We examined differences in the glymphatic system between PFO patients and HCs, and drew a preliminary conclusion. However, longitudinal experiments should be conducted to clarify the effects of time on glymphatic impairment in PFO patients. Notably, we preliminarily enrolled several PFO patients before and after percutaneous interventional closure, and obtained some interesting results. Specifically, using the ALPS index, we found that the glymphatic system function of that PFO patients with severe dysfunction improved after closure; however, it became slightly worse after closure in those with moderate or mild disfunction. Thus, surgeons need to pay more attention to ensure they select effective treatment strategies to reduce the side effects of glymphatic dysfunction. In the future, we intend to recruit patients who suffer from both stroke and PFO. However, we acknowledge that this will not be easy due to the low incidence of the co-morbidity. Additionally, further research with larger sample sizes needs to be conducted to confirm our observations.

Conclusions

This study found that the PFO patients had a significantly decreased DTI-ALPS index, which may indicate disordered ISF dynamics and glymphatic dysfunction. The DTI-ALPS index could serve as a potential neuroimaging biomarker for PFO. These insights extend our understanding of the lymphatic metabolism pathophysiology of PFO. In PFO patients, an impaired glymphatic system before stroke may increase the risk of stroke. Our findings open up new avenues for exploring targeted interventions to mitigate the effects.

Acknowledgments

None.

Footnote

Reporting Checklist: The authors have completed the STROBE reporting checklist. Available at https://qims.amegroups.com/article/view/10.21037/qims-24-1963/rc

Funding: This study was supported by the Key R&D Program Project of Hebei Province (Nos. 21377784D, 20240606, 20230066, and 20210252) and Government Funds Clinical Excellent Medical Talent Training Project of Hebei Province (No. ZF2023149).

Conflicts of Interest: All authors have completed the ICMJE uniform disclosure form (available at https://qims.amegroups.com/article/view/10.21037/qims-24-1963/coif). The authors have no conflicts of interest to declare.

Ethical Statement: The authors are accountable for all aspects of the work in ensuring that questions related to the accuracy or integrity of any part of the work are appropriately investigated and resolved. The study was conducted in accordance with the Declaration of Helsinki

(as revised in 2013). The study was approved by the Institutional Ethics Board of The Second Hospital of Hebei Medical University (No. 2023-R590) and informed consent was taken from all the patients.

References

1. Homma S, Messé SR, Rundek T, Sun YP, Franke J, Davidson K, Sievert H, Sacco RL, Di Tullio MR. Patent foramen ovale. Nat Rev Dis Primers 2016;2:15086.
2. Carroll JD, Saver JL, Thaler DE, Smalling RW, Berry S, MacDonald LA, Marks DS, Tirschwell DL; RESPECT Investigators. Closure of patent foramen ovale versus medical therapy after cryptogenic stroke. N Engl J Med 2013;368:1092-100.
3. Lamy C, Giannesini C, Zuber M, Arquizan C, Meder JF, Trystram D, Coste J, Mas JL. Clinical and imaging findings in cryptogenic stroke patients with and without patent foramen ovale: the PFO-ASA Study. Atrial Septal Aneurysm. Stroke 2002;33:706-11.
4. Blankenship JC. PFO closure: Where are the neurologists? Catheter Cardiovasc Interv 2018;92:187-8.
5. Huber R, Grittner U, Weidemann F, Thijs V, Tanislav C, Enzinger C, Fazekas F, Wolf M, Hennerici MG, McCabe DJ, Putaala J, Tatlisumak T, Kessler C, von Sarnowski B, Martus P, Kolodny E, Norrving B, Rolfs A; . Patent Foramen Ovale and Cryptogenic Strokes in the Stroke in Young Fabry Patients Study. Stroke 2017;48:30-5.
6. Wood KH, Nenert R, Miften AM, Kent GW, Sleyster M, Memon RA, Joop A, Pilkington J, Memon AA, Wilson RN, Catiul C, Szaflarski J, Amara AW. Diffusion Tensor Imaging-Along the Perivascular-Space Index Is Associated with Disease Progression in Parkinson's Disease. Mov Disord 2024;39:1504-13.
7. Sacchi L, D'Agata F, Campisi C, Arcaro M, Carandini T, Örzsik B, Dal Maschio VP, Fenoglio C, Pietroboni AM, Ghezzi L, Serpente M, Pintus M, Conte G, Triulzi F, Lopiano L, Galimberti D, Cercignani M, Bozzali M, Arighi A. A "glympse" into neurodegeneration: Diffusion MRI and cerebrospinal fluid aquaporin-4 for the assessment of glymphatic system in Alzheimer's disease and other dementias. Hum Brain Mapp 2024;45:e26805.
8. Lee DA, Lee HJ, Park KM. Structural connectivity as a predictive factor for responsiveness to levetiracetam treatment in epilepsy. Neuroradiology 2024;66:93-100.
9. Taoka T, Masutani Y, Kawai H, Nakane T, Matsuoka K, Yasuno F, Kishimoto T, Naganawa S. Evaluation of glymphatic system activity with the diffusion MR technique: diffusion tensor image analysis along the perivascular space (DTI-ALPS) in Alzheimer's disease cases. Jpn J Radiol 2017;35:172-8.
10. Mojadidi MK, Zaman MO, Elgendy IY, Mahmoud AN, Patel NK, Agarwal N, Tobis JM, Meier B. Cryptogenic Stroke and Patent Foramen Ovale. J Am Coll Cardiol 2018;71:1035-43.
11. Hayashida K, Fukuchi K, Inubushi M, Fukushima K, Imakita S, Kimura K. Embolic distribution through patent foramen ovale demonstrated by (99m)Tc-MAA brain SPECT after Valsalva radionuclide venography. J Nucl Med 2001;42:859-63.
12. Hansen JM, Charles A. Differences in treatment response between migraine with aura and migraine without aura: lessons from clinical practice and RCTs. J Headache Pain 2019;20:96.
13. Han F, Shirasaki Y, Fukunaga K. Microsphere embolism-induced endothelial nitric oxide synthase expression mediates disruption of the blood-brain barrier in rat brain. J Neurochem 2006;99:97-106.
14. Nozari A, Dilekoz E, Sukhotinsky I, Stein T, Eikermann-Haerter K, Liu C, Wang Y, Frosch MP, Waeber C, Ayata C, Moskowitz MA. Microemboli may link spreading depression, migraine aura, and patent foramen ovale. Ann Neurol 2010;67:221-9.
15. Sánchez-Porras R, Robles-Cabrera A, Santos E. Cortical spreading depolarization: a new pathophysiological mechanism in neurological diseases. Med Clin (Barc) 2014;142:457-62.
16. Vitale M, Tottene A, Zarin Zadeh M, Brennan KC, Pietrobon D. Mechanisms of initiation of cortical spreading depression. J Headache Pain 2023;24:105.
17. Gursoy-Ozdemir Y, Qiu J, Matsuoka N, Bolay H, Bermpohl D, Jin H, Wang X, Rosenberg GA, Lo EH, Moskowitz MA. Cortical spreading depression activates and upregulates MMP-9. J Clin Invest 2004;113:1447-55.
18. Wang W, Redecker C, Bidmon HJ, Witte OW. Delayed neuronal death and damage of GDNF family receptors

in CA1 following focal cerebral ischemia. Brain Res 2004;1023:92-101.
19. Somjen GG. Mechanisms of spreading depression and hypoxic spreading depression-like depolarization. Physiol Rev 2001;81:1065-96.
20. Vinogradova LV, Suleymanova EM, Medvedeva TM. Transient loss of interhemispheric functional connectivity following unilateral cortical spreading depression in awake rats. Cephalalgia 2021;41:353-65.
21. Vigna C, Marchese N, Inchingolo V, Giannatempo GM, Pacilli MA, Di Viesti P, Impagliatelli M, Natali R, Russo A, Fanelli R, Loperfido F. Improvement of migraine after patent foramen ovale percutaneous closure in patients with subclinical brain lesions: a case-control study. JACC Cardiovasc Interv 2009;2:107-13.
22. Saengjaroentham C, Supornsilpchai W, Ji-Au W, Srikiatkhachorn A, Maneesri-le Grand S. Serotonin depletion can enhance the cerebrovascular responses induced by cortical spreading depression via the nitric oxide pathway. Int J Neurosci 2015;125:130-9.
23. Beda RD, Gill EA Jr. Patent foramen ovale: does it play a role in the pathophysiology of migraine headache? Cardiol Clin 2005;23:91-6.
24. SUN L, CHU T, WANG Y, WANG X. Radiolabeling and biodistribution of a nasopharyngeal carcinoma-targeting peptide identified by in vivo phage display. Acta Biochim Biophys Sin (Shanghai) 2007;39:624-32.
25. Globus MY, Wester P, Busto R, Dietrich WD. Ischemia-induced extracellular release of serotonin plays a role in CA1 neuronal cell death in rats. Stroke 1992;23:1595-601.
26. Du B, Yu J, Zhou ZL, Zhang P, Yu M, Qian M. Selection of the peptides specifically binding to hepatoma by using phage display in vivo. Zhonghua Zhong Liu Za Zhi 2005;27:645-7.
27. Guo ZN, Xing Y, Liu J, Wang S, Yan S, Jin H, Yang Y. Compromised dynamic cerebral autoregulation in patients with a right-to-left shunt: a potential mechanism of migraine and cryptogenic stroke. PLoS One 2014;9:e104849.
28. Chen S, Shao L, Ma L. Cerebral Edema Formation After Stroke: Emphasis on Blood-Brain Barrier and the Lymphatic Drainage System of the Brain. Front Cell Neurosci 2021;15:716825.
29. Wang YJ, Sun YR, Pei YH, Ma HW, Mu YK, Qin LH, Yan JH. The lymphatic drainage systems in the brain: a novel target for ischemic stroke? Neural Regen Res 2023;18:485-91.
30. Iliff JJ, Wang M, Liao Y, Plogg BA, Peng W, Gundersen GA, Benveniste H, Vates GE, Deane R, Goldman SA, Nagelhus EA, Nedergaard M. A paravascular pathway facilitates CSF flow through the brain parenchyma and the clearance of interstitial solutes, including amyloid β. Sci Transl Med 2012;4:147ra111.
31. Jessen NA, Munk AS, Lundgaard I, Nedergaard M. The Glymphatic System: A Beginner's Guide. Neurochem Res 2015;40:2583-99.
32. Carare RO, Bernardes-Silva M, Newman TA, Page AM, Nicoll JA, Perry VH, Weller RO. Solutes, but not cells, drain from the brain parenchyma along basement membranes of capillaries and arteries: significance for cerebral amyloid angiopathy and neuroimmunology. Neuropathol Appl Neurobiol 2008;34:131-44.
33. Aspelund A, Antila S, Proulx ST, Karlsen TV, Karaman S, Detmar M, Wiig H, Alitalo K. A dural lymphatic vascular system that drains brain interstitial fluid and macromolecules. J Exp Med 2015;212:991-9.
34. Harrison IF, Ismail O, Machhada A, Colgan N, Ohene Y, Nahavandi P, Ahmed Z, Fisher A, Meftah S, Murray TK, Ottersen OP, Nagelhus EA, O'Neill MJ, Wells JA, Lythgoe MF. Impaired glymphatic function and clearance of tau in an Alzheimer's disease model. Brain 2020;143:2576-93.
35. Lundgaard I, Lu ML, Yang E, Peng W, Mestre H, Hitomi E, Deane R, Nedergaard M. Glymphatic clearance controls state-dependent changes in brain lactate concentration. J Cereb Blood Flow Metab 2017;37:2112-24.
36. Christensen J, Yamakawa GR, Shultz SR, Mychasiuk R. Is the glymphatic system the missing link between sleep impairments and neurological disorders? Examining the implications and uncertainties. Prog Neurobiol 2021;198:101917.
37. Taoka T, Naganawa S. Imaging for central nervous system (CNS) interstitial fluidopathy: disorders with impaired interstitial fluid dynamics. Jpn J Radiol 2021;39:1-14.
38. El Husseini N, Katzan IL, Rost NS, Blake ML, Byun E, Pendlebury ST, Aparicio HJ, Marquine MJ, Gottesman RF, Smith EE; . Cognitive Impairment After Ischemic and Hemorrhagic Stroke: A Scientific Statement From the American Heart Association/American Stroke Association. Stroke 2023;54:e272-91.
39. Tarasoff-Conway JM, Carare RO, Osorio RS, Glodzik L, Butler T, Fieremans E, Axel L, Rusinek H, Nicholson C, Zlokovic BV, Frangione B, Blennow K, Ménard J, Zetterberg H, Wisniewski T, de Leon MJ. Clearance systems in the brain--implications for Alzheimer diseaser. Nat Rev Neurol 2016;12:248.
40. Papadopoulos MC, Manley GT, Krishna S, Verkman AS.

Aquaporin-4 facilitates reabsorption of excess fluid in vasogenic brain edema. FASEB J 2004;18:1291-3.
41. van Veluw SJ, Hou SS, Calvo-Rodriguez M, Arbel-Ornath M, Snyder AC, Frosch MP, Greenberg SM, Bacskai BJ. Vasomotion as a Driving Force for Paravascular Clearance in the Awake Mouse Brain. Neuron 2020;105:549-561.e5.
42. Wang M, Ding F, Deng S, Guo X, Wang W, Iliff JJ, Nedergaard M. Focal Solute Trapping and Global Glymphatic Pathway Impairment in a Murine Model of Multiple Microinfarcts. J Neurosci 2017;37:2870-7.
43. Wardlaw JM, Smith C, Dichgans M. Small vessel disease: mechanisms and clinical implications. Lancet Neurol 2019;18:684-96.
44. Jiang-Xie LF, Drieu A, Bhasiin K, Quintero D, Smirnov I, Kipnis J. Neuronal dynamics direct cerebrospinal fluid perfusion and brain clearance. Nature 2024;627:157-64.
45. Tian S, Hong H, Luo X, Zeng Q, Huang P, Zhang M. Association between body mass index and glymphatic function using diffusion tensor image-along the perivascular space (DTI-ALPS) in patients with Parkinson's disease. Quant Imaging Med Surg 2024;14:2296-308.
46. Zhu H, Xie Y, Li L, Liu Y, Li S, Shen N, Zhang J, Yan S, Liu D, Li Y, Zhu W. Diffusion along the perivascular space as a potential biomarker for glioma grading and isocitrate dehydrogenase 1 mutation status prediction. Quant Imaging Med Surg 2023;13:8259-73.
47. Guo Y, Wu L, Liu J, Liu J, Sun Z. Correlation between glymphatic dysfunction and cranial defect in severe traumatic brain injury: a retrospective case-control study based on a diffusion tensor image analysis along the perivascular space (DTI-ALPS) investigation. Quant Imaging Med Surg 2024;14:6756-66.
48. Ji C, Yu X, Xu W, Lenahan C, Tu S, Shao A. The role of glymphatic system in the cerebral edema formation after ischemic stroke. Exp Neurol 2021;340:113685.
49. Zhu J, Mo J, Liu K, Chen Q, Li Z, He Y, Chang Y, Lin C, Yu M, Xu Y, Tan X, Huang K, Pan S. Glymphatic System Impairment Contributes to the Formation of Brain Edema After Ischemic Stroke. Stroke 2024;55:1393-404.
50. Hlauschek G, Nicolo JP, Sinclair B, Law M, Yasuda CL, Cendes F, Lossius MI, Kwan P, Vivash L. Role of the glymphatic system and perivascular spaces as a potential biomarker for post-stroke epilepsy. Epilepsia Open 2024;9:60-76.
51. Lv T, Zhao B, Hu Q, Zhang X. The Glymphatic System: A Novel Therapeutic Target for Stroke Treatment. Front Aging Neurosci 2021;13:689098.
52. Toh CH, Siow TY. Glymphatic Dysfunction in Patients With Ischemic Stroke. Front Aging Neurosci 2021;13:756249.
53. Chao X, Fang Y, Lu Z, Wang J, Yin D, Shi R, Wang P, Liu X, Sun W. Impairments of neurovascular coupling after stroke lower glymphatic system function and lead to depressive symptom: A longitudinal cohort study. J Affect Disord 2024;367:255-62.
54. Keuters MH, Antila S, Immonen R, Plotnikova L, Wojciechowski S, Lehtonen S, Alitalo K, Koistinaho J, Dhungana H. The Impact of VEGF-C-Induced Dural Lymphatic Vessel Growth on Ischemic Stroke Pathology. Transl Stroke Res 2024. [Epub ahead of print]. doi: 10.1007/s12975-024-01262-9.
55. Dobs K, Martinez J, Kell AJE, Kanwisher N. Brain-like functional specialization emerges spontaneously in deep neural networks. Sci Adv 2022;8:eabl8913.
56. Güntürkün O, Ströckens F, Ocklenburg S. Brain Lateralization: A Comparative Perspective. Physiol Rev 2020;100:1019-63.
57. Rogers LJ. Brain Lateralization and Cognitive Capacity. Animals (Basel) 2021.
58. Vogelsang DA, Furman DJ, Nee DE, Pappas I, White RL 3rd, Kayser AS, D'Esposito M. Dopamine Modulates Effective Connectivity in Frontal Cortex. J Cogn Neurosci 2024;36:155-66.
59. Wei DY, O'Daly O, Zelaya FO, Goadsby PJ. Areas of cerebral blood flow changes on arterial spin labelling with the use of symmetric template during nitroglycerin triggered cluster headache attacks. Neuroimage Clin 2022;33:102920.
60. Taoka T, Ito R, Nakamichi R, Nakane T, Kawai H, Naganawa S. Diffusion Tensor Image Analysis ALong the Perivascular Space (DTI-ALPS): Revisiting the Meaning and Significance of the Method. Magn Reson Med Sci 2024;23:268-90.
61. Ringstad G. Glymphatic imaging: a critical look at the DTI-ALPS index. Neuroradiology 2024;66:157-60.
62. Smith EE, Greenberg SM. Beta-amyloid, blood vessels, and brain function. Stroke 2009;40:2601-6.
63. Dyke JP, Xu HS, Verma A, Voss HU, Chazen JL. MRI characterization of early CNS transport kinetics post intrathecal gadolinium injection: Trends of subarachnoid and parenchymal distribution in healthy volunteers. Clin Imaging 2020;68:1-6.
64. Naganawa S, Ito R, Nakamichi R, Kawamura M, Taoka T, Yoshida T, Sone M. Relationship between Time-dependent Signal Changes in Parasagittal Perivenous Cysts and

Leakage of Gadolinium-based Contrast Agents into the Subarachnoid Space. Magn Reson Med Sci 2021;20:378-84.
65. Barisano G, Sepehrband F, Collins HR, Jillings S, Jeurissen B, Taylor JA, et al. The effect of prolonged spaceflight on cerebrospinal fluid and perivascular spaces of astronauts and cosmonauts. Proc Natl Acad Sci U S A 2022;119:e2120439119.
66. Li Y, Zhou Y, Zhong W, Zhu X, Chen Y, Zhang K, He Y, Luo Z, Ran W, Sun J, Lou M. Choroid Plexus Enlargement Exacerbates White Matter Hyperintensity Growth through Glymphatic Impairment. Ann Neurol 2023;94:182-95.

Cite this article as: Sun L, Cui K, Hu J, Dong L, Liu L, Jia J, Yu J, Yang J. Impaired glymphatic system in patent foramen ovale based on diffusion tensor imaging analysis along the perivascular space. Quant Imaging Med Surg 2025;15(4):2987-2999. doi: 10.21037/qims-24-1963